Preliminary observations of a high-strain zone along the western flank of the Galore Creek deposit area, northwestern British Columbia

Russell Johnston[1, a], Lori Kennedy[1], and Bram I. van Straaten[2]

[1] Department of Earth, Ocean and Atmospheric Sciences, The University of British Columbia, Vancouver, BC, V6T 1Z4
[2] British Columbia Geological Survey, Ministry of Energy, Mines and Low Carbon Innovation, Victoria, BC, V8W 9N3
[a] corresponding author: rjohnston@eoas.ubc.ca

Recommended citation: Johnston, R., Kennedy, L., and van Straaten, B.I., 2023. Preliminary observations of a high-strain zone along the western flank of the Galore Creek deposit area, northwestern British Columbia. In: Geological Fieldwork 2022, British Columbia Ministry of Energy, Mines and Low Carbon Innovation, British Columbia Geological Survey Paper 2023-01, pp. 51-63.

Abstract

The 1.4 Bt Galore Creek Cu-Au porphyry deposit is hosted in a Late Triassic alkalic silica-undersaturated volcano-intrusive complex. The deposit is bordered to the west by a 2-3 km wide, >6 km long, poorly understood, foliated, and folded zone (here termed the Butte ridge deformation zone) juxtaposed against the deposit by faults. The deformation zone records anomalously high strain in Stuhini Group rocks compared to elsewhere in the Galore Creek area, and its origin is enigmatic. Previous workers have considered the zone as mylonitic or a zone of flattening. Based on three 1:5000-scale transects across Butte ridge, we divide the area into seven fault-bounded structural domains. Our preliminary observations of changes in fold geometry and foliation intensity coupled with consistent southward fold plunges suggest that west-dipping thrust faults juxtaposed rocks in these domains from different structural levels. The lowest apparent strain and presumably shallowest structural level is in domain 7, east of the deformation zone and in the footwall of the Saddle thrust and Butte fault. In the northern domains (1 and 2), folds are typically open and show a well-developed axial planar pressure solution cleavage; beds maintain a constant layer thickness typical of parallel folds, which tend to form under relatively low-temperature conditions. Farther south, in domains 3 and 6, all folds are tight to isoclinal and have the thickened hinges of similar folds that typically form under higher temperatures, and the rocks display a well-developed bedding-parallel cleavage. We consider that deeper structural levels are exposed southward, with rocks in domain 6 having formed at the greatest depth. We interpret that the Butte ridge area records strain by fold and foliation development rather than by non-coaxial strain along discrete shear zones. Local examples of non-coaxial strain were likely produced due to slip as a fold mechanism. Future work will assess the absolute and relative timing of deformation and determine the relationship between deformation and mineralization.

Keywords: Alkalic porphyry Cu-Au, Galore Creek, Stuhini Group, deformation, strain

1. Introduction

Galore Creek is a large alkalic silica-undersaturated porphyry Cu-Au-Ag deposit in northwestern British Columbia (Fig. 1) on the traditional lands of the Tahltan First Nation. The deposit is bounded to the west by a north-striking deformation zone (here called the Butte ridge deformation zone) that is several km wide and at least 6 km long (Fig. 2). The deformation zone has been described as mylonitic (Enns et al., 1995; Logan, 2005), a folded corridor (Schwab et al., 2008; Micko et al., 2014; Febbo, 2019), and the site of weak metamorphism (Micko et al., 2014). Enns et al. (1995) considered that the zone is cut by alteration and mineralization. If true, deformation must be younger than the age of the host rocks (<210 Ma, van Straaten et al., 2023) and older than the age of mineralization (>210-208.5 Ma; Mortensen et al., 1995; Logan and Mihalynuk, 2014), suggesting broadly syn-mineralization deformation. The Butte ridge deformation zone records higher strain than that observed in the deposit, and the origin of the deformation is not well understood.

Here, we present preliminary field observations on the lithology, structural style, and kinematics of the Butte ridge deformation zone. Ongoing studies will address the timing and physical conditions (P, T) of deformation in the Galore Creek area, the relationship of deformation to mineralization and to regional deformation events. Our long-term goal is to unravel the latest Triassic to recent deformation history of the Galore Creek area, with a focus on the timing and style of deformation and their relationship to the emplacement and post-emplacement modification of the Galore Creek alkalic porphyry Cu-Au system.

2. Geological setting

2.1. Regional geology

The Galore Creek area is in the Stikine island arc terrane (Stikinia), which consists of three volcano-sedimentary packages: the Stikine assemblage (Devonian to Permian), the Stuhini Group (Upper Triassic) and the Hazelton Group (uppermost Triassic to Middle Jurassic). These successions are separated by unconformities associated with deformation in the Permo-Triassic (Logan and Koyanagi, 1994), latest Triassic (e.g., Nelson et al., 2022) and Middle Jurassic (Mihalynuk et al., 1994; Nelson et al., 2013). Accretion of

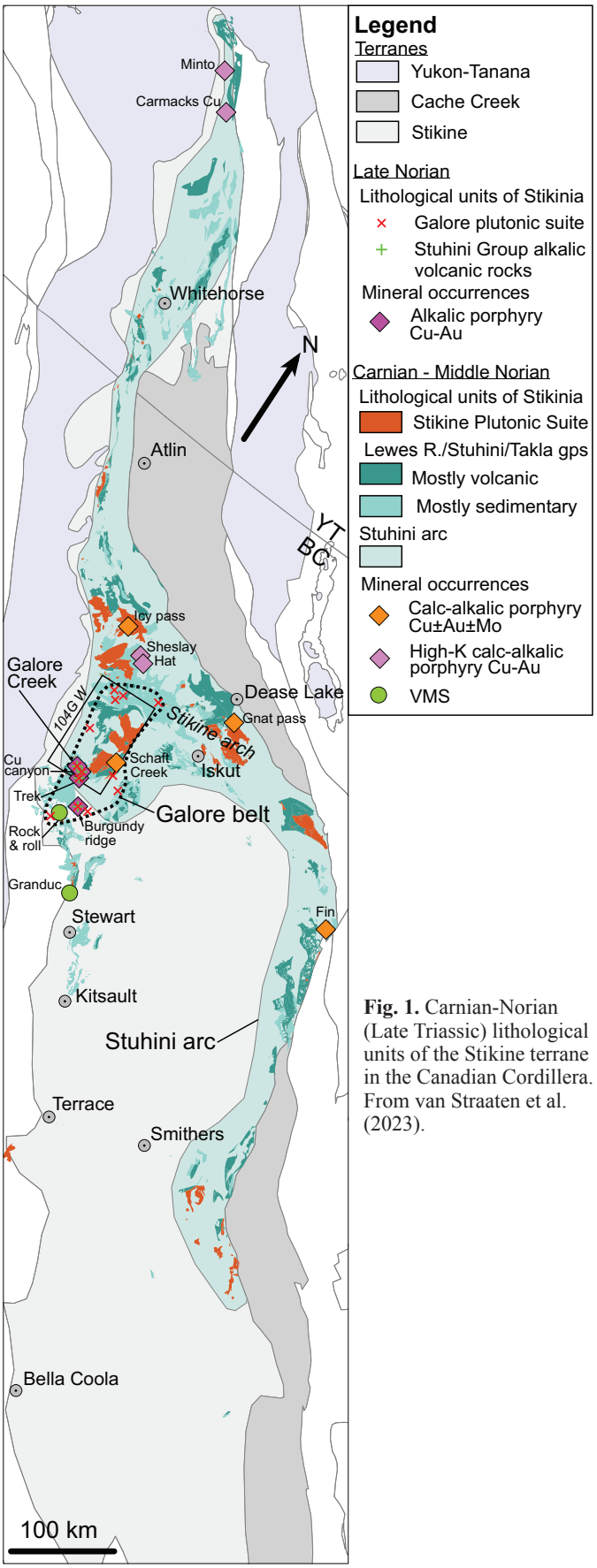

Fig. 1. Carnian-Norian (Late Triassic) lithological units of the Stikine terrane in the Canadian Cordillera. From van Straaten et al. (2023).

Stikinia to Ancestral North America is recorded by deposition of Bowser Lake Group siliciclastic rocks (Middle Jurassic to mid-Cretaceous) in a foreland basin atop Stikinia (Evenchick et al., 2007). Bowser Lake Group and older rocks are deformed by Cretaceous Skeena folding and thrusting linked to continued convergence between accreted terranes and Ancestral North America (Evenchick et al., 2007). Bowser basin displays a thin-skinned folding and thrusting structural style. In the older rocks of Stikinia, which are more competent than the sedimentary rocks of the Bowser Basin, strain tends to be partitioned into narrow zones of folding and faulting controlled by pre-existing structures, or local less competent horizons (Febbo et al., 2019; Nelson and van Straaten, 2020). Two generations of folds have been associated with Cretaceous deformation. Northwest-trending, orogen-parallel folds are predominant in the Bowser basin although distinct sets of northeast-trending folds are also present. Northwest-trending folds are thought to have formed from orogen-normal shortening, and northeast-trending folds due to orogen-parallel shortening (Evenchick, 2001; Evenchick et al., 2007). Late Cretaceous dextral faults and Paleocene-Eocene dextral transtensional faults are documented throughout the region. Eocene deformation may have reactivated earlier faults (Nelson et al., 2013).

The Stuhini arc (Late Triassic) contains thick accumulations of predominantly mafic volcanic strata and 229-216 Ma Stikine Plutonic Suite intrusions. These volcanic and intrusive rocks extend for at least 1300 km along the northeastern margin of the Stikine terrane (Fig. 1) and have been interpreted as an east-facing arc (Nelson and van Straaten, 2020). Stuhini arc activity was terminated in latest Triassic by a collision between northern Stikinia and the Yukon-Tanana terrane. This collision is expressed, in part, by latest Triassic shortening of the Stuhini Group and older strata throughout northwestern British Columbia (Henderson et al., 1992; Rhys, 1993; Brown et al., 1996; Rees et al., 2015; Nelson et al., 2018). In addition, recent studies of the collision (Colpron et al., 2022; Nelson et al., 2022) suggest the alkalic magmatism responsible for the Galore plutonic suite occurred during the early stages of Yukon-Tanana - Stikinia collision (van Straaten et al., 2023).

2.2. Geology of the Galore Creek area

The oldest rocks in the Galore Creek area are in the hanging wall of the west-verging Copper canyon thrust, and comprise Stikine assemblage limestone (Permian) and fine-grained siliciclastic rocks (Lower-Middle Triassic; Logan and Koyanagi, 1994; Fig. 2). Elsewhere, the study area is underlain by Stuhini Group volcano-sedimentary rocks (Upper Triassic). Stuhini Group strata are cut by the Galore plutonic suite (Enns et al., 1995; Fig. 2). The age range of alkalic silica-undersaturated intrusions is broadly constrained by a 210 ±1 Ma U-Pb titanite and K-feldspar age for an early syn-mineralization K-feldspar and pseudoleucite porphyritic syenite intrusion (Mortensen et al., 1995) and a 208.5 ±0.8 Ma U-Pb titanite age for a K-feldspar porphyritic biotite quartz syenite plug (Logan and Mihalynuk, 2014) interpreted by Enns et al. (1995) as the youngest Galore intrusions.

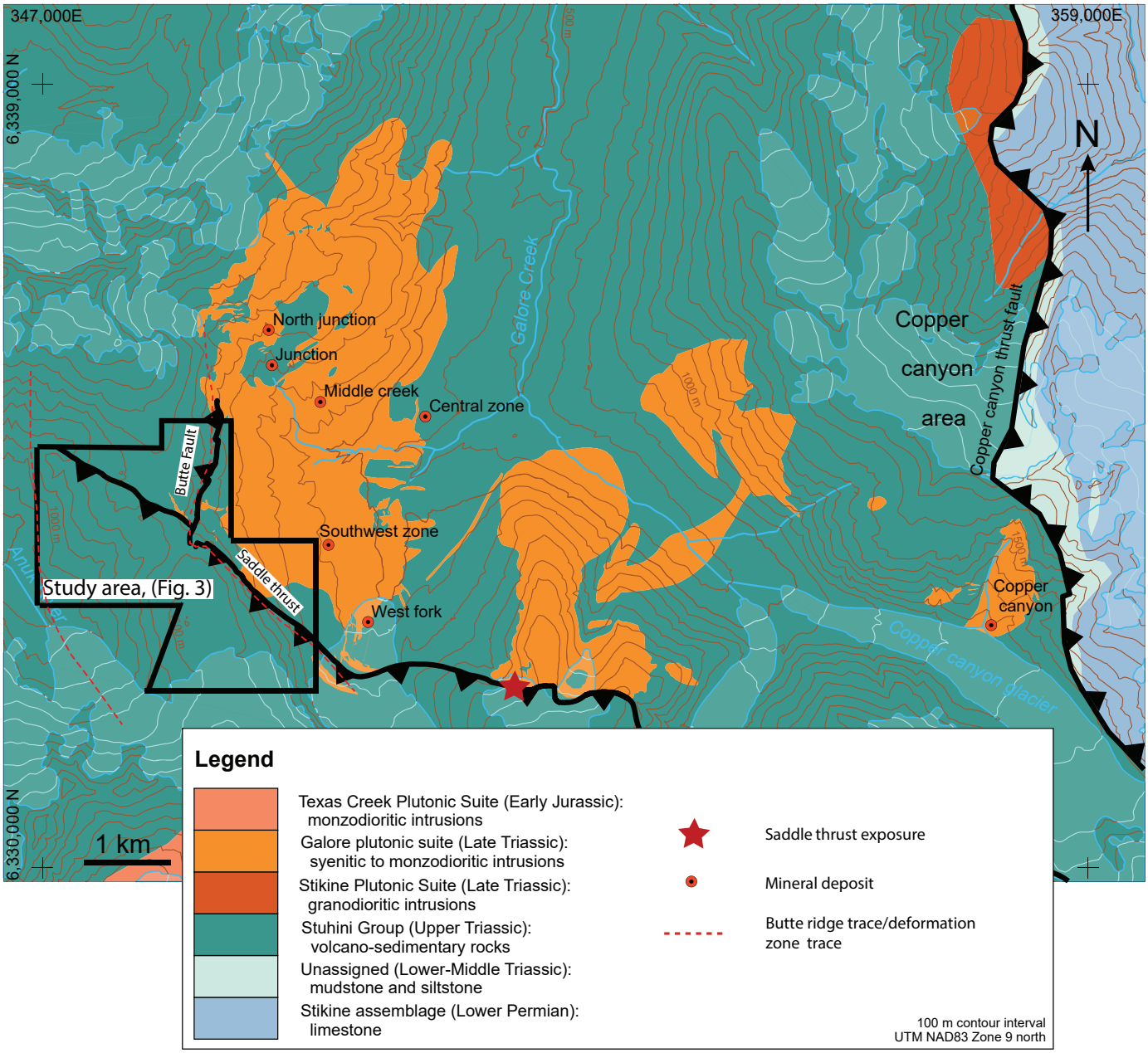

Fig. 2. Geology of the Galore Creek area. Modified from van Straaten et al. (2023); location of Saddle and Butte thrusts based on 2022 mapping. UTM coordinates here and throughout this paper are in NAD83 zone 9 north.

Penetrative planar fabrics are common in Paleozoic and Middle Triassic strata. However, penetrative deformation of Upper Triassic and younger rocks is rare, restricted to north-trending zones of foliation, such as the Butte ridge deformation zone (Figs. 2, 3; Febbo, 2019; Micko et al., 2014). Logan and Koyanagi (1994) documented post-Triassic southward-vergent structures that are overprinted by post-Jurassic northerly trending folds and thrusts in the Stuhini Group and younger rocks. Brittle deformation is widespread, including map-scale reverse faults (e.g., east-verging Saddle and Butte thrusts; west-verging Canyon Creek thrust, Fig. 2) and outcrop-scale thrusts. Dextral and sinistral fault zones are common; they crosscut the main foliation and are defined by offset units.

3. Butte ridge stratigraphy

We carried out detailed (1:5000 scale) mapping of Butte ridge along three cross-strike transects (Figs. 3, 4) that we refer to as 'northern' (section A-A'), central (section B-B'), and southern (section C-C'). Stuhini Group subunits and map unit codes described below mainly follow van Straaten et al. (2023).

3.1. Stuhini Group (Upper Triassic)

van Straaten et al. (2023) subdivided the Stuhini Group in the Galore Creek area into a lower intermediate to mafic volcano-sedimentary succession and an upper alkalic volcanic succession.

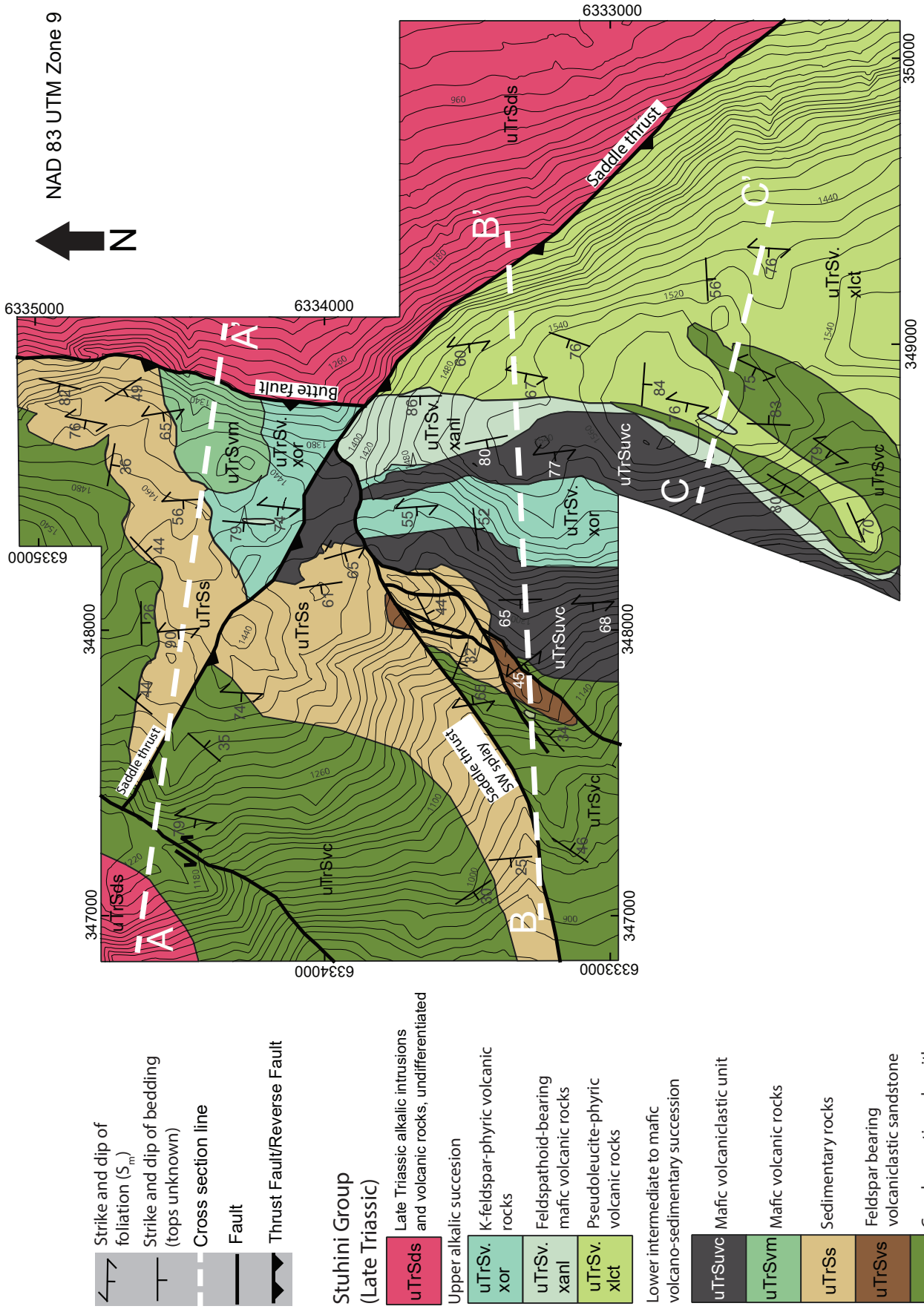

Fig. 3. Geology of the Butte ridge deformation zone. Cross section lines A-A', B-B', C-C' are shown on Figure 4.

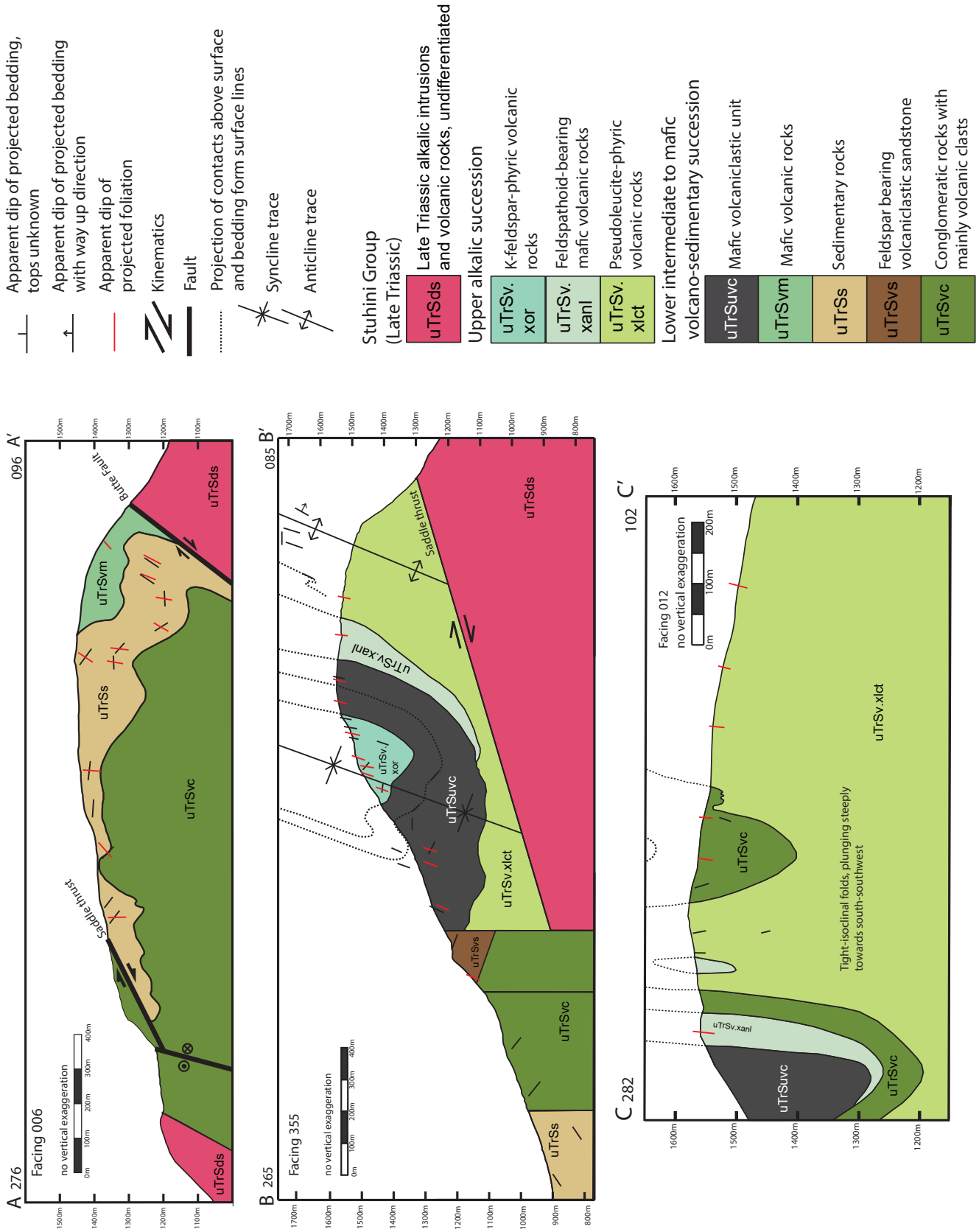

Fig. 4. Cross sections across Butte ridge. **a)** A-A' **b)** B-B', **c)** C-C'. See Figure 3 for locations.

3.1.1. Lower intermediate to mafic volcano-sedimentary succession

At the base of the section is a commonly well-bedded (cm-m scale) conglomeratic unit (uTrSvc) containing white-weathering, pebble to cobble amphibole-porphyritic igneous clasts and sparser other volcanic clasts (Fig. 5a). Where a fabric is well-developed, the matrix is generally chloritized. The white-weathering clasts are commonly aligned in the main foliation plane (S_m). Some have internal extension fractures perpendicular to S_m; some clasts appear broken, with segments displaced along internal fractures oblique to S_m (Fig. 5a). The unit is exposed on the northern and western margins of the map area and locally on the southern margin (Fig. 3). It is locally interbedded with narrow lenses of augite-phyric mafic volcanic rocks (similar to unit uTrSvm, see below). A well-bedded feldspar (plagioclase?)-bearing volcaniclastic sandstone unit (uTrSvs) overlies uTrSvc in two small areas and may be a lateral equivalent of unit uTrSs (see below).

The volcanic clast-bearing conglomerate unit (uTrSvc) is overlain by a sedimentary unit (uTrSs) containing siltstone, sandstone, conglomerate, and limestone. Sandstones and siltstones may define sharp-based fining-upward sequences (Fig. 5b). Sandstones and conglomerates are typically massive and rarely show bedding. This unit is in the northern and western parts of the map area. The lower contact with the volcanic clast-bearing conglomerate unit was not directly observed; the location of the contact is constrained to <30 m in the east, but unconstrained in the west.

A mafic volcanic unit (uTrSvm) contains clasts with 20-40% euhedral-subhedral augite crystals (up to 5 mm) and locally elongate plagioclase crystals (<5 mm) in an aphanitic groundmass (Fig. 5c). This unit is restricted to the northeastern part of the map area (Fig. 3) and was not observed elsewhere.

A distinct feldspathoid-bearing mafic volcanic unit (uTrSvm.xanl) is commonly found as m- to dam-scale lenses in units uTrSv.xor, uTrSv.xlct, and uTrSvm. As much as 150 m is present at the western contact of uTrSv.xlct. The distinctive phenocrysts are white spheroidal minerals, interpreted as feldspathoids. The crystals are typically 0.5-3 mm and range from 15-75% of the rock by volume (Fig. 6a). Augite phenocrysts are locally present. The groundmass is dark grey and aphanitic. This unit is interpreted as transitional between the lower intermediate to mafic volcano-sedimentary succession and the upper alkalic volcanic succession.

The mafic volcaniclastic unit (uTrSuvc) consists of volcanic-derived siltstone, sandstone, and conglomerate (Fig. 6b). The unit was not mapped north of the Saddle thrust fault. Clasts in the conglomerate range from pebbles to cobbles and are typically mafic. The volcanic clasts commonly contain fine augite(?) and feldspar crystals. The unit is similar to uTrSvc but lacks the diagnostic white-weathering amphibole-phyric clasts of uTrSvc. The two volcaniclastic sequences appear to occupy different stratigraphic positions. Although pseudoleucite-bearing clasts seem to be lacking, uTrSuvc appears to be between uTrSvm.xanl and uTrSv.xor (see below).

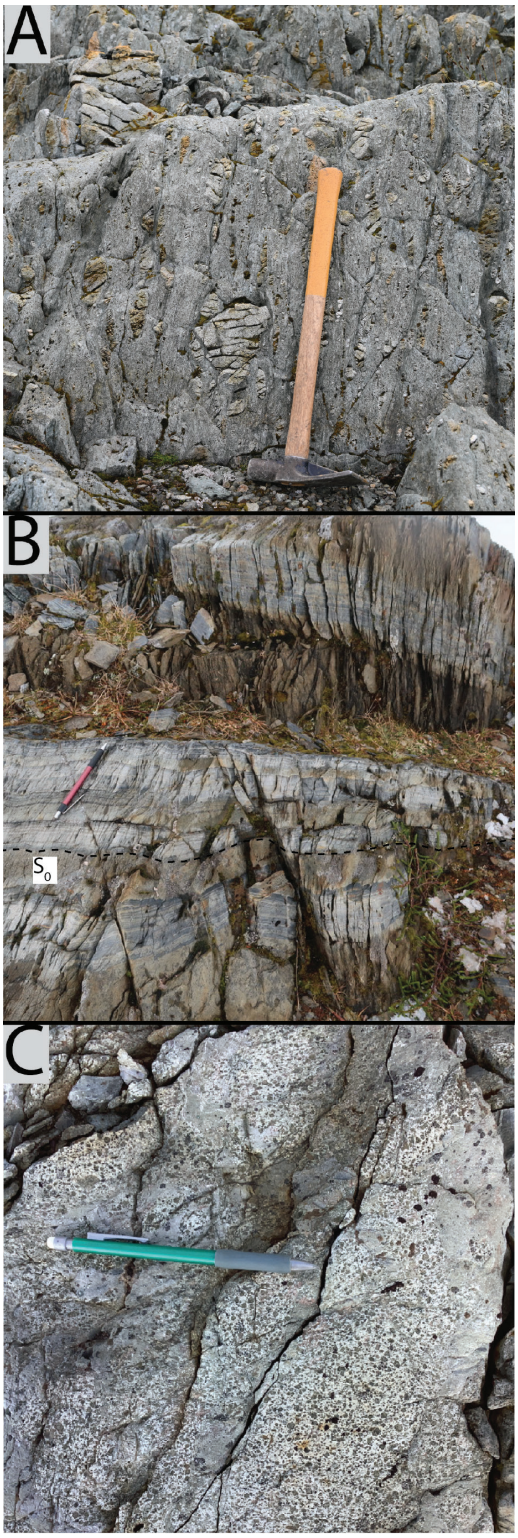

Fig. 5. Lower intermediate to mafic volcano-sedimentary succession. **a)** Unit uTrSvc with a well-developed chloritic foliation (S_m); some white-weathering clasts have internal extension fractures normal to the foliation, some clasts appear broken, with slip along shear fractures oblique to S_m (348641E, 6332288N). **b)** Unit uTrSs well-bedded siltstone and sandstone with sharp-based fining upward sequences and a well-developed pressure solution cleavage (S_m). Bedding is orthogonal to cleavage, indicating a fold hinge (348009E, 6334548N). **c)** uTrSvm with coarse augite phenocrysts (346430E, 6335567N).

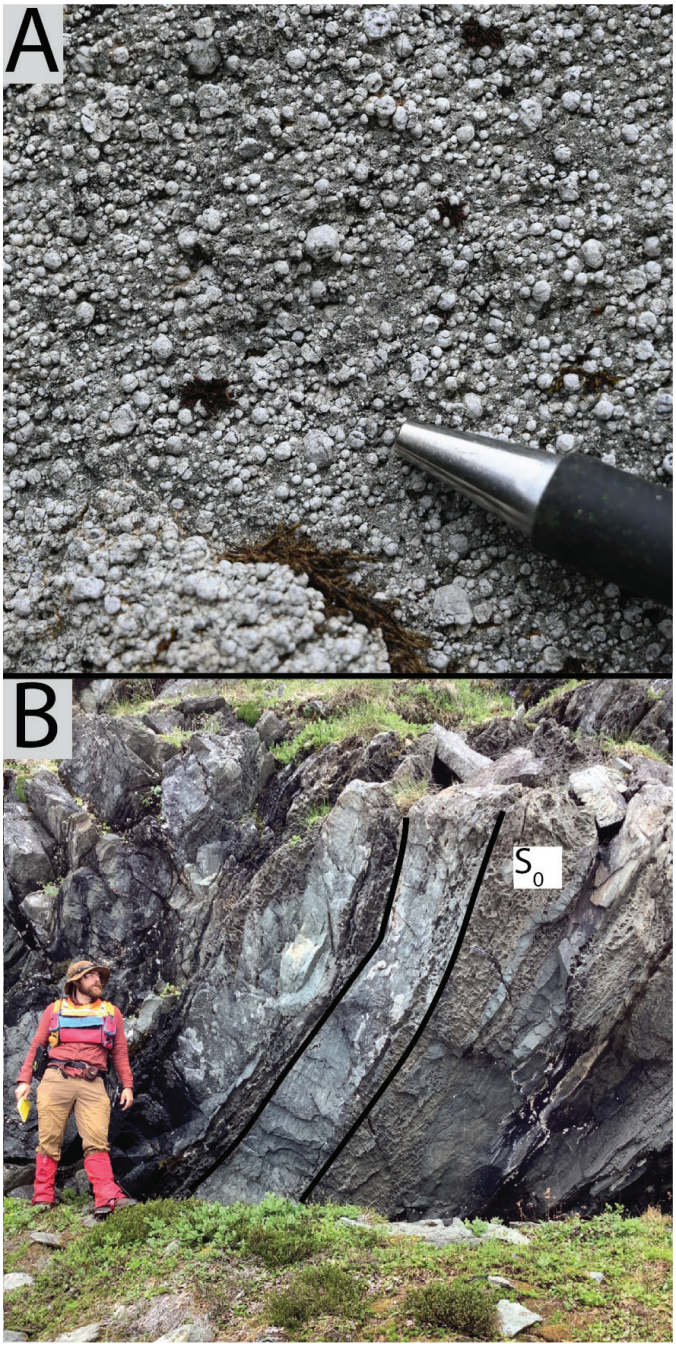

Fig. 6. Rock units in the central transect. **a)** uTrSvm.xanl, crystal tuff facies with white-weathering spheroidal feldspathoid crystals (348613E, 6332657N). **b)** Unit uTrSuvc volcaniclastic, siltstone and sandstone facies (348082E, 6333247N).

3.1.2. Upper alkalic volcanic succession

Capping the mafic volcaniclastic unit uTrSuvc is a pseudoleucite-phyric volcanic unit (uTrSv.xlct); pseudoleucite phenocrysts are diagnostic of the unit. Here, pseudoleucite refers to any mineral or aggregate of minerals that originated as a leucite crystal. Pseudoleucite crystals may be black and set in a light-toned groundmass (Fig. 7a) or white weathering in a dark grey to black groundmass (Fig. 7b). The unit may contain good bedding, defined by tuffaceous interbeds or variation in

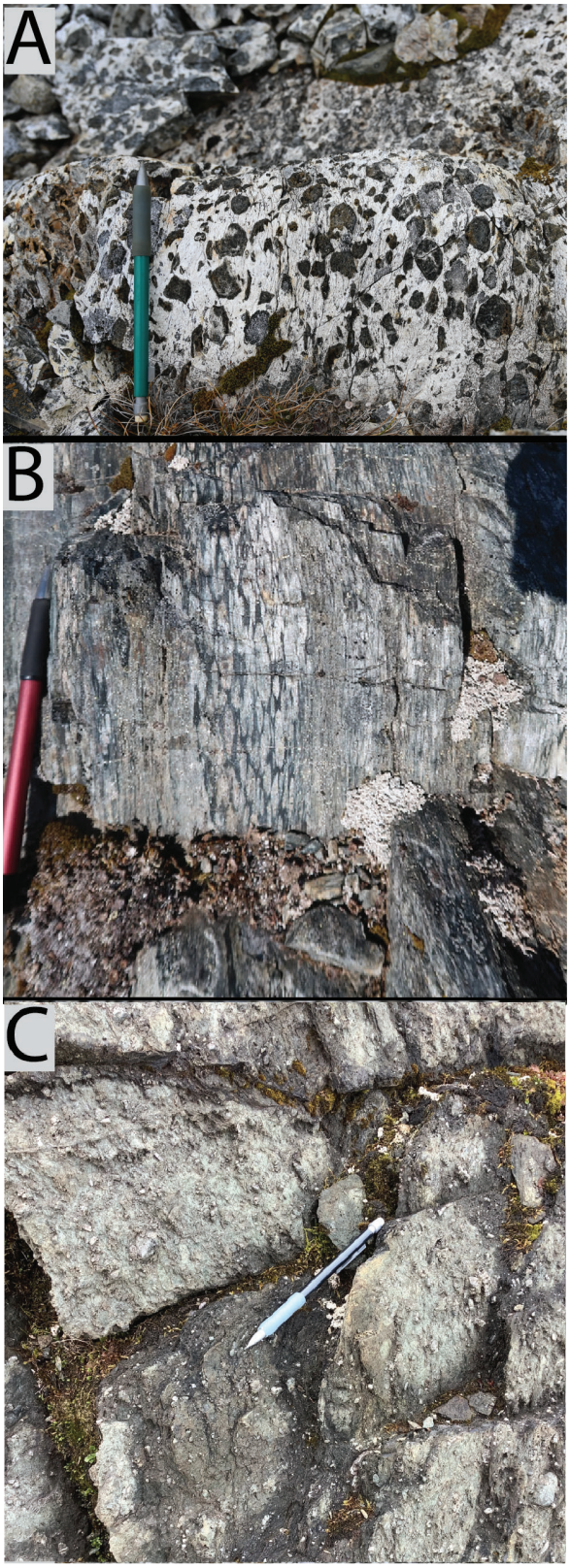

Fig. 7. Upper alkalic volcanic succession rocks. **a)** Coarse, zoned, and broken pseudoleucite-bearing uTrSv.xlct (349189E, 6332688N). **b)** Bedded and flattened pseudoleucite-bearing uTrSv.xlct. Foliation is parallel to bedding (348866E, 3333267N). **c)** uTrSmv.xor, crystal tuff facies with coarse (>1 cm) broken euhedral K-feldspar crystals (348472E, 6333298N).

pseudoleucite crystal size and abundance. In some areas, the unit is massive with up to 35% 1-3 cm broken pseudoleucite crystals in a grey uniform groundmass. The pseudoleucite-phyric volcanic unit is the most voluminous lithology at surface in the map area but is spatially restricted to the southeast (Fig. 3).

A K-feldspar-phyric volcanic unit (uTrSv.xor) contains diagnostic tabular, generally euhedral, and broken K-feldspar crystals, <1 mm to >3 cm long (most commonly >0.5 cm; Fig. 7c). A wide range of volcanic facies are observed, with significant variation in crystal abundances and grain size distributions. The unit is most abundant in the central transect but is locally mapped in the northern transect.

3.2. Galore plutonic suite and undifferentiated Late Triassic alkalic volcanic rocks

Rocks in the footwall of the Saddle and Butte thrust faults consist of altered and mineralized Late Triassic volcanic rocks and intrusions. The intrusions are Late Triassic and range from syenitic to monzodioritic. The alkalic intrusions typically contain distinct K-feldspar phenocryst and/or pseudoleucite phenocrysts. For detailed descriptions, see Enns et al. (1995).

4. Study area deformation

The Butte ridge deformation zone (Fig. 2) contains the most strained Stuhini Group rocks in the area. However, deformation intensity is variable both across and along strike. Folds are common and have a poorly to well-developed axial planar foliation. Crenulation cleavages are common; they are steeply and shallowly dipping, with both steep and shallowly plunging fold axes, and a wide range of orientations. The crenulations fold the main foliation. Crenulation intensity varies with location; rocks in the hanging wall of the Saddle thrust are the most crenulated.

Penetrative folding and cleavage development records coaxial flattening or 'pure shear' (Fig. 8); non-coaxial or 'simple shear' strain is rare in the Butte ridge deformation zone. Relatively incompetent sedimentary and volcaniclastic rocks typically have a well-developed foliation whereas more competent rocks do not. Pseudoleucite-bearing rocks locally exhibit extreme strain partitioning in texturally homogenous rocks over a m- to dm-scale, with some units strongly flattened and others weakly flattened.

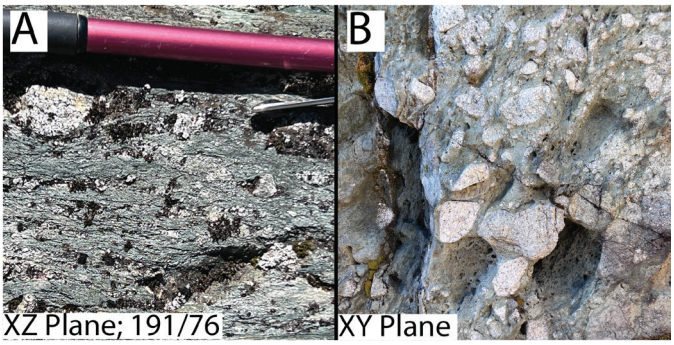

Fig. 8. Different views of the S_m fabric at the same outcrop; unit uTrSvc. **a)** Photo taken perpendicular to the XZ plane of the strain ellipse, showing a well-developed fabric defined by flattened clasts in chlorite-rich matrix. **b)** View looking down on the plane of flattening of the strain ellipse (XY plane). In this plane, the clasts are not elongate, indicating that the foliation is a flattening foliation related to folding, with no evidence of stretching (e.g., shearing) (347399E, 6334542N).

Brittle faults, both outcrop scale and map scale are abundant. Along strike and across strike of the Butte ridge deformation zone, brittle faults separate areas with distinct deformation styles, that we separate into structural domains (Fig. 9). Below, we first describe the faults that bound these domains and then we describe the deformation features within each domain.

4.1. Brittle faults

Two major thrust faults (Butte and Saddle, Figs. 3, 4) are in the area; minor thrusts are common throughout the Butte ridge deformation zone (Fig. 10). The Butte fault is a north-trending structure that defines the eastern boundary of the Butte ridge deformation zone in the northern part of the study area. The fault juxtaposes the deformation zone against Galore plutonic suite intrusions and/or strongly hydrothermally altered rocks (Fig. 3). At the surface, the fault is a 5-6 m wide light-toned band, exposed for 100s of m along strike. Due to steep topography, the fault was only accessible in one area, where it is exposed as a zone >10 m wide within which are strips of fault gouge (<0.5 m wide) between bands of more coherent but brecciated rock. Reverse motion is not confirmed by stratigraphic offset or kinematics from within the fault zone. Using drill core intersections, the fault is estimated as moderately to steeply west dipping. It is unclear if S_m and the Butte fault are cogenetic or if the fault is a later structure.

The Saddle thrust fault (118°/34°, where measured) trends northwest for a >8 km strike length across the Butte Ridge deformation zone, juxtaposing the volcanic conglomerate unit (uTrSvc) over siltstones, sandstones, and conglomerates of unit (uTrSs). The thrust contains abundant quartz veins in the footwall and a 1-5 m deformation zone consisting of numerous faults splays (Febbo, 2019). At Butte ridge, the Saddle thrust splays into at least two distinct segments. One splay, along a topographic lineament in the southwest part of the map area ('Saddle thrust southwest splay', Fig. 3), is defined by an abrupt change in lithology, bedding orientation, and foliation intensity. The main fault extends into the northwestern portion of the map area ('Saddle thrust northwest', Fig. 3) and is inferred on the basis of a pronounced topographic lineament, an abrupt change in lithology from uTrSvc to uTrSs, a sharp decrease in foliation intensity from east to west, an abrupt change in bedding orientation, and abundant quartz veins in the footwall. The amount of offset on these fault segments is unclear. The Saddle thrust appears to truncate the Butte thrust.

4.2. Structural domains

The Butte fault, the Saddle thrust and two interpreted northeast-trending faults on the western side of the central transect define separate domains of distinct structural style

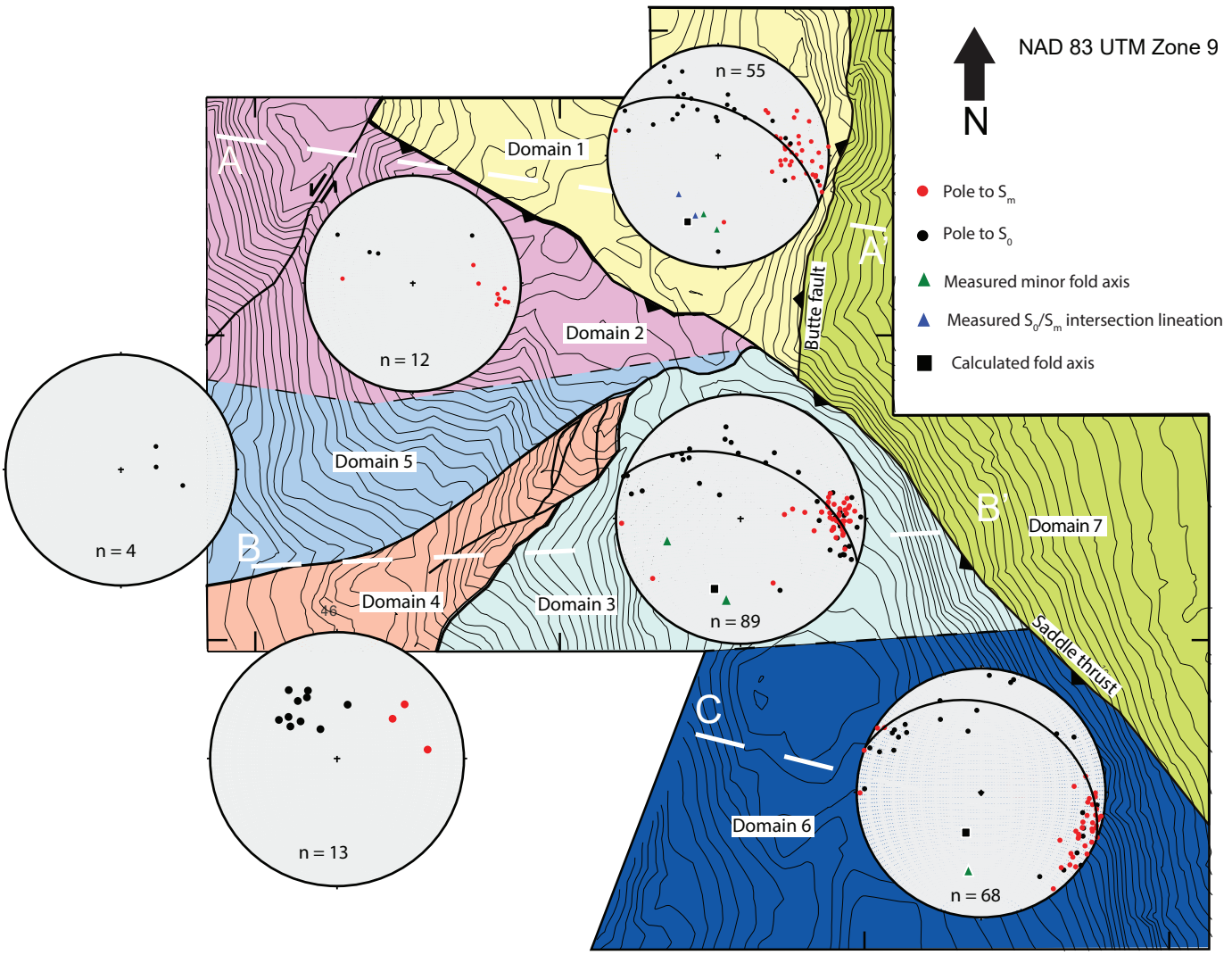

Fig. 9. Structural domains and lower hemisphere equal-area stereographic projections of the Butte deformation zone. Calculated F_2 fold axes: domain 1, 205/35°; domain 3, 200/40°; domain 6, 201/62°. Stereonets and β calculations were produced using Stereonet 11 (Allmendinger et al., 2013; Cardozo and Allmendinger, 2013). Colours do not imply stratigraphy and are used only to highlight the domains.

and/or structural orientation (domains 1-9, Fig. 9). Below we describe these domains within each transect from east to west across Butte ridge, focussing on penetrative strain and folds. Minor brittle faults and veins are common in all domains but do not change character between domains.

4.2.1. Domain 1

This domain is a fault block bounded by the Butte fault to the east and the Saddle thrust to the west (Figs. 3, 9). Folds with wavelengths ranging from 10 cm to 1 km generally have an open, and rarely close, geometry. Axial surfaces are steeply inclined to the west and fold axes are gently to moderately plunging to the south-southwest (β calculation, 206°/35°; Fig. 9). Bedding thicknesses are generally constant indicating that these are parallel folds (Class 1B of Ramsay, 1967). Sedimentary rocks can have a strong axial planar pressure solution cleavage (S_m, Fig. 5b); volcaniclastic rocks have moderately developed axial planar cleavage defined by chlorite (Fig. 5b). Cleavage orientations show significant variation, with an average orientation of 180°/64°. Rare intrafolial folds have smaller wavelengths (<10 cm) than described above. The folds have a tight to isoclinal geometry and have a similar fold profile with thickened hinges (Fig. 11; Class 2 of Ramsay, 1967).

Map scale folds on the eastern side of this fault block are gentle to open and asymmetric, with long limbs dipping steeply to the east (northern transect, Fig. 4a) and record an easterly vergence. Bedding orientation shallows towards the center of the fault block and is interpreted as a hinge zone to a km-scale fold. Foliation intensity in this domain is greatest on the eastern margin, near the Butte fault, and gradually weakens to the west. Near the Saddle thrust, the rocks are weakly to non-foliated. From west to east there is a progressive decrease in the angles between the fold axial surfaces and S_m and the Butte fault (Fig. 4a).

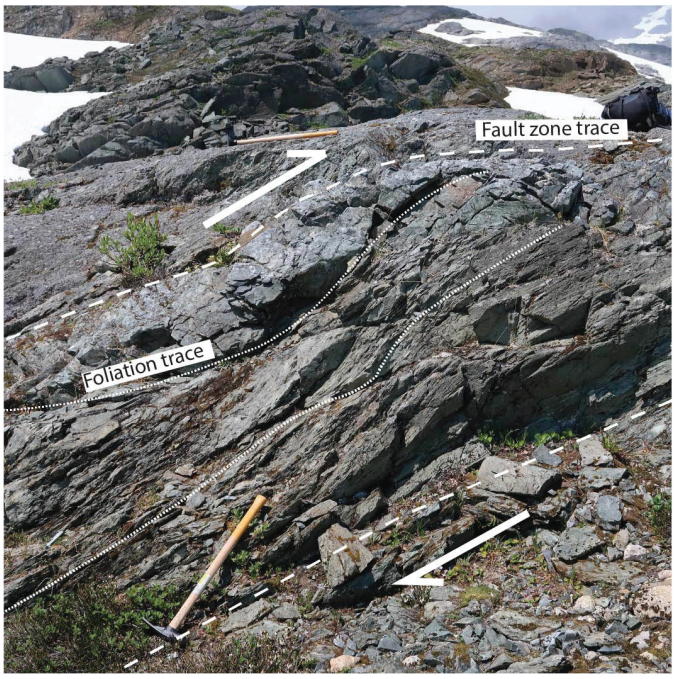

Fig. 10. Minor thrust fault in the Butte deformation zone showing top-to-east kinematics. It is unclear if S_m formed before the fault or if the fault and S_m are cogenetic (348850E, 6334768N).

Fig. 11. Tight to isoclinal similar intrafolial folds in domain 1 tuffs (348449E, 6334484N).

4.2.2. Domain 2

Most of this fault-bounded domain consists of the volcanic clast-bearing conglomerate unit (uTrSvc). Rocks in the hanging wall of the Saddle thrust are highly strained relative to those in the immediate footwall. Unit uTrSvc has a well-developed north-trending steeply dipping cleavage defined by chlorite; more competent igneous clasts display internal fractures (Fig. 5a). Foliation intensity is strongest close to the Saddle thrust, but has the same general orientation as in domain 1 across the fault.

4.2.3. Domain 3

Domain 3 is bounded by the Saddle thrust to the east and an unnamed inferred fault to the west (Fig. 9). The domain shows a different style of folds than observed in domain 1 to the north. Folds are close to tight, with steeply inclined west-dipping axial surfaces, and have gentle to moderate south-southwest plunges (β calculation, 200°/40°; Figs. 9, 12). Folds have wavelengths of <1 m to 500 m and verge to the east. A map-scale east-vergent synform-antiform pair is on the eastern side of domain 3 (Fig. 4b).

The eastern portion of this domain is mainly underlain by pseudoleucite-bearing rocks (uTrSv.xlct). A strong fabric (S_m) is present throughout, typically defined by chlorite and by alignment of clasts and pseudoleucite crystals. Flattened pseudoleucite grains can have aspect ratios of 2:1 to 10:1 (Fig. 7b). However, adjacent pseudoleucite-phyric coherent rocks can be largely undeformed, illustrating extreme strain gradients. The S_m fabric is commonly parallel to bedding and, similar to the northern transect, dips steeply to the west.

Fig. 12. Close folds in unit uTrSv.xlct (348997E, 6333035N).

4.2.4. Domain 4

This domain is separated from domain 3 by a northeast-trending fault across which bedding orientation and foliation intensity changes abruptly. Bedding in this fault block consistently dips 35-50° to the southeast (Fig. 9). Foliation intensity is weaker than in domain 3 and decreases to the west. In the easternmost part of the fault block, weak foliations were

mapped in two locations, dipping moderately to the southeast. On western edge of the fault block, a fabric is locally developed in carbonate-bearing clasts (lenses?), but the host rock is not foliated (Fig. 13).

4.2.5. Domain 5

Domain 5 is separated from domain 4 by an interpreted splay off the Saddle thrust. Bedding in domain 5 dips gently-moderately to the west and this fault is interpreted based on the sharp change in bedding orientation and lithology. Siltstones and volcaniclastic rocks in this domain are not foliated.

4.2.6. Domain 6

Tight to isoclinal south-plunging (β calculation, 201°/66°; Fig. 9) folds are common throughout this area and are well-exposed at the m- to dam-scale (Fig. 14). Unlike the northern domains, where folds verge to the east, the isoclinal folds do not show vergence (Fig. 4c). Rocks generally have a well-defined S_m foliation defined by chlorite alignment, aligned clasts, and local pressure solution cleavage. In this domain, pseudoleucite-phyric volcanic rocks are locally strongly foliated, with the foliation defined by flattened pseudoleucite crystals that locally display a stretching lineation; aspect ratio 1:8). Rock types with black pseudoleucite crystals in a light-toned groundmass display significantly less flattening strain (aspect ratios of 1:1 to 1:4) than rock types with white pseudoleucite crystals in a dark-toned groundmass (aspect ratio 1:2).

An outcrop displaying dm-scale type 3 fold interference pattern is exposed at the southern edge of this domain in a volcanic tuff, where isoclinal F_1 folds with the S_m foliation are overprinted by later tight folds lacking a foliation (Fig. 15). The hinge of the tight later fold is thickened relative to the limbs. This type of refolding was not observed elsewhere on Butte ridge but was observed 8 km along strike to the north. In the southern part of the domain S_m foliation is oriented 233°/86°, in the northern part of the domain, foliation is oriented 188°/83°.

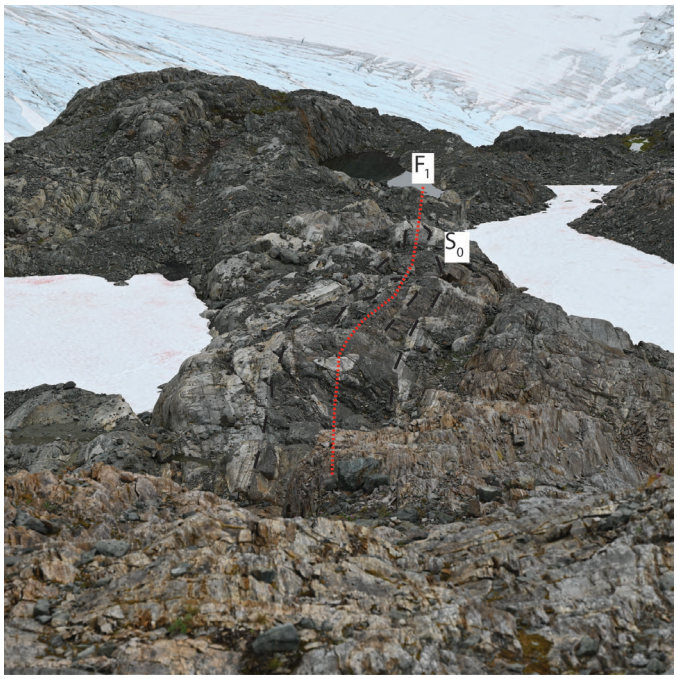

Fig. 14. Decametre-scale isoclinal fold in domain 6. The light-toned unit(s) are tuffaceous beds. View to the south (348483E, 6332228N).

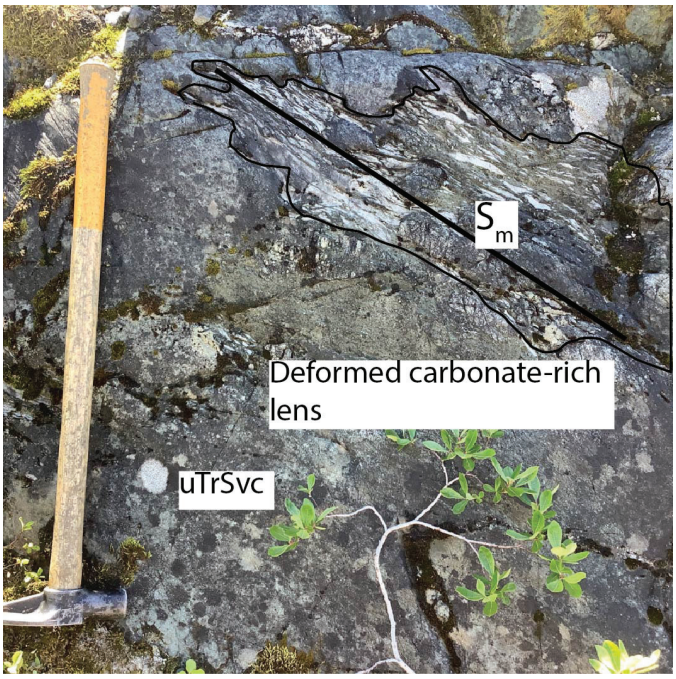

Fig. 13. Flattening fabric in carbonate-bearing clast (lens?) in otherwise unfoliated uTrSmv (347234E, 6333134N).

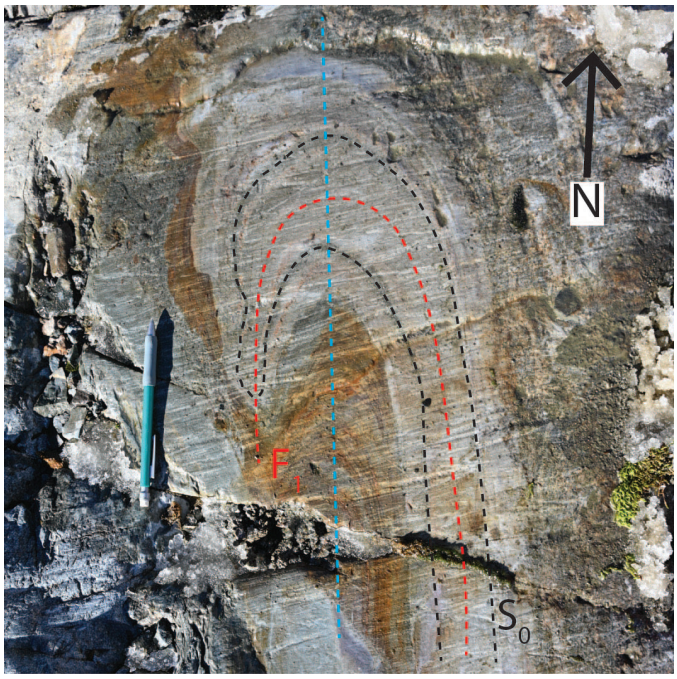

Fig. 15. Type 3 fold interference pattern in volcanic tuff. Early folds are isoclinal and have a layer-parallel foliation, later folds are tight (348405E, 6332151N).

4.2.7. Domain 7

The easternmost domain is in the footwall of the Saddle thrust and Butte faults. The domain is underlain by the Galore plutonic suite intrusive rocks and highly altered and locally mineralized volcanic rocks. Rocks in this fault block are generally unfoliated but are strongly faulted and locally folded (Febbo, 2019).

5. Discussion

The Butte ridge area consists of a series of fault-bounded folded domains, where fold geometry and orientation change from north to south. In the northern domains, folds are typically open and, more rarely, close and show a well-developed axial planar cleavage. Fold axial surfaces generally dip steeply to the west and the folds plunge gently to moderately south-southwest. A pressure solution cleavage is typical, and beds maintain a constant layer thickness, typical of parallel folds (class 1B of Ramsay, 1967). Such folds tend to form under relatively low temperatures typical of thin-skinned fold and thrust belts. We interpret that the area records strain by fold and foliation development rather than by non-coaxial strain along discrete shear zones. Local examples of non-coaxial strain were likely produced due to slip as a fold mechanism.

In the central domains, map-scale folds are generally steeply inclined, east verging, and plunge gently to moderately to the south-southwest. Although most folds are tight, open to close profiles were observed. Bedding and cleavage are parallel except at fold hinges. In domain 6, all folds are tight to isoclinal. The folds have the thickened hinges of similar folds (class 2 of Ramsay, 1967) typically associated with higher temperature deformation. Rocks display a well-developed bedding-parallel cleavage, and a stretching lineation was noted at one locality. Locally, outcrop-scale coaxial fold interference was observed, with an isoclinal fold containing a bedding-parallel foliation being tightly refolded into a type 3 (Ramsay, 1967) hook displaying a similar fold profile. We interpret the southern domain to represent the highest strain on the ridge.

Preliminary observations suggest that changes in deformation style and strain intensity are a result of faulting that has juxtaposed rocks from different structural levels, presumably along west- or southwest-dipping faults. We interpret that the shallowest structural level in the area is in the footwall of the Saddle and Butte faults (domain 7, Fig. 9). Based on fold geometry, foliation intensity, and consistent southward fold plunges, we consider that deeper structural levels are exposed between the Saddle and Butte faults (domain 1) and still deeper levels farther south, with rocks in domain 6 recording the deepest structural level.

We are uncertain how folds and fabrics in the study area relate to the regional geology, and the absolute timing of the Saddle and Butte thrusts is unclear. The structures may be related to latest Triassic regional shortening or Cretaceous development of the Skeena fold and thrust belt, or both. Future work will aim to establish both the absolute and relative timing of the structures and to place the area into a regional structural framework.

Enns et al. (1995) considered that the deformation zone is cut by alteration and mineralization. If true, deformation must be younger than the age of the host rocks (<210 Ma, van Straaten et al., 2023) and older than the age of Galore Creek porphyry Cu-Au-Ag mineralization (>210-208.5 Ma; Mortensen et al., 1995; Logan and Koyanagi, 1994; Logan, 2004), suggesting a broadly syn-mineralization deformation event. We did not see with confidence cross-cutting relationships between alteration/mineralization and deformation that would constrain the relative timing.

6. Summary

Galore Creek is a large alkalic silica-undersaturated porphyry Cu-Au-Ag deposit in northwestern British Columbia. The deposit area is bounded to the west by a north-striking deformation zone (here called the Butte ridge deformation zone) that is several km wide and at least 6 km long. The deformation zone contains the most strained Stuhini Group rocks in the Galore area (Logan and Koyanagi, 1994; Micko et al., 2014; Febbo, 2019) consisting of folded rocks with moderately to strongly developed axial planar cleavage. We propose that progressively deeper structural levels, separated by faults, are exposed from north to south along the Butte ridge.

Acknowledgments

Funding for this research was provided by a Department of Natural Resources Geoscience Targeted GeoSciences Initiative grant to Lori Kennedy and Bram van Straaten. We thank Galore Creek Mining Corporation for their generous logistical support; Leif Bailey, Nils Peterson, Well-Shen Lee, and other colleagues for discussions and camaraderie at camp. Thanks to Gayle Febbo and Jim Logan for sharing with us their knowledge and insight of the (complicated) Galore Creek geology. An internal report and geological maps of the area by Gayle Febbo, Jim Logan and Esther Bordet were valuable resources. We thank Jim Logan for a helpful review of the manuscript. Thanks to William Raleigh-Smith for providing capable and cheerful field assistance.

References cited

Allmendinger, R.W., Cardozo, N., and Fisher, D., 2012. Structural geology algorithms: Vectors and tensors in structural geology. Cambridge University Press, 289 p.

Brown, D.A., Gunning, M.H., and Greig, C.J., 1996. The Stikine project: Geology of western Telegraph Creek map area, northwestern British Columbia. British Columbia Ministry of Employment and Investment, British Columbia Geological Survey Bulletin 95, 130 p.

Cardozo, N., and Allmendinger, R.W., 2013. Spherical projections with OSXStereonet. Computers & Geosciences, 51, 193-205.

Colpron, M., Sack, P.J., Crowley, J.L., Beranek, L.P., and Allan, M.M., 2022. Late Triassic to Jurassic magmatic and tectonic evolution of the Intermontane terranes in Yukon, northern Canadian Cordillera: Transition from arc to syn-collisional magmatism and post-collisional lithospheric delamination. Tectonics, 41, article e2021tc007060, doi:10.1029/2021TC007060.

Enns, S.G., Thompson, J.F.H., Stanley, C.R., and Yarrow, E.W., 1995. The Galore Creek porphyry copper-gold deposits, northwestern British Columbia. In: Schroeter, T.G., (Ed.), Porphyry Deposits of the Northern Cordillera. Canadian Institute of Mining and Metallurgy Special Volume 46, pp. 630-644.

Evenchick, C.A., 2001. Northeast-trending folds in the western Skeena Fold Belt, northern Canadian Cordillera: A record of Early Cretaceous sinistral plate convergence. Journal of Structural Geology, 23, 1123-1140.

Evenchick, C.A., McMechan, M.E., McNicoll, V.J., and Carr, S.D., 2007. A synthesis of the Jurassic-Cretaceous tectonic evolution of the central and southeastern Canadian Cordillera: Exploring links across the orogen. In: Sears, J.W., Harms, T.A., and Evenchick, C.A., (Eds.), Whence the Mountains? Inquiries into the Evolution of Orogenic Systems: A Volume in Honor of Raymond A. Price. Geological Society of America Special Paper 443, pp. 117-145.

Febbo, G., 2019. Galore Creek geology map. In: Prince, J., 2019, Drilling, Geological Mapping, and Aerial Survey Assessment Report on the Galore Creek Project. British Columbia Geological Survey Assessment Report number 39156, Appendix XIV.

Febbo, G.E., Kennedy, L.A., Nelson, J.L., Savell, M.J., Campbell, M.E., Creaser, R.A., Friedman, R.M., van Straaten, B.I., and Stein, H.J., 2019. The evolution and structural modification of the supergiant Mitchell Au-Cu porphyry, northwestern British Columbia. Economic Geology, 114, 303-324.

Henderson, J.R., Kirkham, R.V., Henderson, M.N., Payne, J.G., Wright, T.O., and Wright, R.L., 1992. Stratigraphy and structure of the Sulphurets area, British Columbia. In: Current Research Part A, Cordillera and Pacific Margin, Geological Survey of Canada, Paper 92-1A, pp. 323-332.

Lang. J.R., Lueck, B., Mortensen, J.K., Russell, J.K., Stanley, C.R., and Thompson, J.F.H., 2005. Triassic-Jurassic silica-undersaturated and silica-saturated alkalic intrusions in the Cordillera of British Columbia: Implications for arc magmatism. Geology, 23, 451-454.

Logan, J.M., 2005. Alkaline magmatism and porphyry Cu-Au deposits at Galore Creek, northwestern British Columbia. In: Geological Fieldwork 2004, British Columbia Ministry of Energy, Mines and Petroleum Resources, British Columbia Geological Survey Paper 2005-01, pp. 237-248.

Logan, J.M., and Koyanagi, V.M., 1994. Geology and mineral deposits of the Galore Creek area. British Columbia Ministry of Energy, Mines and Petroleum Resources, British Columbia Geological Survey, Bulletin 92, 102 p.

Logan, J.M., and Mihalynuk, M.G., 2014. Tectonic controls on Early Mesozoic paired alkaline porphyry deposit belts (Cu-Au ±Ag-Pt-Pd-Mo) within the Canadian Cordillera. Economic Geology, 109, 827-858.

Micko, J., Tosdal, R.M., Bissig, T., Chamberlain, C.M., and Simpson, K.A., 2014. Hydrothermal alteration and mineralization of the Galore Creek alkalic Cu-Au porphyry deposit, northwestern British Columbia, Canada. Economic Geology, 109, 891-914.

Mihalynuk, M.G., Nelson, J., and Diakow, L.J., 1994. Cache Creek terrane entrapment: Oroclinal paradox within the Canadian Cordillera. Tectonics, 13, 575-595.

Mortensen, J.K., Ghosh, D.K., and Ferri, F., 1995. U-Pb geochronology of intrusive rocks associated with copper-gold porphyry deposits in the Canadian Cordillera. In: Schroeter, T.G., (Ed.), Porphyry Deposits of the Northwestern Cordillera of North America. Canadian Institute of Mining, Metallurgy and Petroleum, Special Volume 46, pp. 142-158.

Nelson, J., and Kyba, J., 2014. Structural and stratigraphic control of porphyry and related mineralization in the Treaty Glacier-KSM-Brucejack-Stewart trend of western Stikinia. In: Geological Fieldwork 2013, British Columbia Ministry of Energy, Mines and Petroleum Resources, British Columbia Geological Survey Paper 2014-1, pp. 111-140.

Nelson, J., Waldron, J., van Straaten, B., Zagoresvski, A., and Rees, C., 2018. Revised stratigraphy of the Hazelton Group in the Iskut River region, northwestern British Columbia. In: Geological Fieldwork 2017, British Columbia Ministry of Energy, Mines and Petroleum Resources, British Columbia Geological Survey Paper 2018-1, pp. 15-38.

Nelson, J.L., and van Straaten, B., 2020. Recurrent syn- to post-subduction mineralization along deep crustal corridors in the Iskut-Stewart-Kitsault region of western Stikinia, northwestern British Columbia. In: Sharman, E.R., Lang, J.R., and Chapman, J.B., (Eds.), Porphyry Deposits of the Northwestern Cordillera of North America: A 25-Year Update. Canadian Institute of Mining and Metallurgy Special Volume 57, pp. 194-211.

Nelson, J.L., van Straaten, B., and Friedman, R., 2022. Latest Triassic-Early Jurassic Stikine-Yukon-Tanana terrane collision and the onset of accretion in the Canadian Cordillera: Insights from Hazelton Group detrital zircon provenance and arc-back-arc configuration. Geosphere, 18, 670-696.

Nelson, J.L., Colpron, M., and Israel, S., 2013. The Cordillera of British Columbia, Yukon and Alaska: Tectonics and metallogeny. In: Colpron, M., Bissig, T., Rusk, B.G., and Thompson, J., (Eds.), Tectonics, Metallogeny and Discovery: The North American Cordillera and Similar Accretionary Settings, Society of Economic Geologists Special Publication 17, pp. 53-110.

Ramsay, J.G., 1967. Folding and fracturing of rocks: McGraw-Hill Book Company, New York, 560 p.

Rees, C., Riedell, K.B., Proffett, J.M., Macpherson, J., and Robertson, S., 2015. The Red Chris porphyry copper-gold deposit, northern British Columbia, Canada: Igneous phases, alteration, and controls of mineralization. Economic Geology, 110, 857-888.

Rhys, D.A., 1993. Geology of the Snip Mine, and its relationship to the magmatic and deformational history of the Johnny Mountain area, northwestern British Columbia. M.Sc. thesis, The University of British Columbia, Vancouver, B.C., Canada. Available from <https://circle.ubc.ca/handle/2429/2173> accessed April 12, 2012.

Schwab, D.L., Petsel, S., Otto, B.R., Morris, S.K., Workman, E., and Tosdal, R.M., 2008. Overview of the Late Triassic Galore Creek copper-gold-silver porphyry system. In: Spencer, J.E., and Titley, S.R., (Eds.), Arizona Geological Society Digest 22, pp. 1-14.

van Straaten, B.I., Friedman, R.M., and Camacho, A., 2023. Stratigraphy of the Stuhini Group (Upper Triassic) in the Galore Creek area, northwestern British Columbia. In: Geological Fieldwork 2022, British Columbia Ministry of Energy, Mines and Low Carbon Innovation, British Columbia Geological Survey Paper 2023-01, pp. 33-49.